

Article

A Novel Approach for the Biological Desalination of Major Anions in Seawater Using Three Microalgal Species: A Kinetic Study

Madeha O. I. Ghobashy ^{1,2,*}, Omar Bahattab ¹ , Aishah Alatawi ¹, Meshari M. Aljohani ³ 
and Mohamed M. I. Helal ^{4,*}

- ¹ Biology Department, Faculty of Science, University of Tabuk, Tabuk 71421, Saudi Arabia; obahattab@ut.edu.sa (O.B.); amm.alatawi@ut.edu.sa (A.A.)
² Microbiology Department, Faculty of Science, Ain Shams University, Cairo 11566, Egypt
³ Chemistry Department, Faculty of Science, University of Tabuk, Tabuk 71421, Saudi Arabia; mualjohani@ut.edu.sa
⁴ National Research Centre, Chemistry of Natural and Microbial Products Department, Pharmaceutical and Drug Industries Division, Cairo 11566, Egypt
* Correspondence: mghobashy@ut.edu.sa (M.O.I.G.); dmohamedhelal@yahoo.com (M.M.I.H.)

Abstract: The global water shortage alert has been upgraded to a higher risk level. Consequently, a sustainable approach for ecofriendly, energy efficient water desalination is required for agricultural and municipal water reuse. In this study, an energy-efficient biological desalination process was used to treat chloride anions, which are the most abundant anion salt in seawater. Three algal species were studied: *Scenedimsmus arcuatus* (*S. arcuatus*), *Chlorella vulgaris* (*C. vulgaris*), and *Spirulina maxima* (*Sp. maxima*), under different operating conditions (saline concentrations, contact time, high light intensity, and CO₂ supply), and two kinetic models were used. It was identified that under a high light intensity and CO₂ supply, *S. arcuatus* enhanced chloride removal from 32.42 to 48.93%; the daily bioaccumulation capacity (Q_e), according to the kinetic models, was enhanced from 124 to 210 mg/g/day; and the net biomass production was enhanced from 0.02 to 0.740 g/L. The EDX analysis proved that salt bioaccumulation may be attributed to the replacement of Ca²⁺ and Mg²⁺ with Na⁺ and K⁺ through algal cells. The study's findings provide promising data that can be used in the search for novel energy-efficient alternative ecofriendly desalination technologies based on algae biological systems with biomass byproducts that can be reused in a variety of ways.



Citation: Ghobashy, M.O.I.; Bahattab, O.; Alatawi, A.; Aljohani, M.M.; Helal, M.M.I. A Novel Approach for the Biological Desalination of Major Anions in Seawater Using Three Microalgal Species: A Kinetic Study. *Sustainability* **2022**, *14*, 7018. <https://doi.org/10.3390/su14127018>

Academic Editors: Abdelkader T. Ahmed and Md. Shafiquzzmaan

Received: 5 May 2022

Accepted: 31 May 2022

Published: 8 June 2022

Publisher's Note: MDPI stays neutral with regard to jurisdictional claims in published maps and institutional affiliations.



Copyright: © 2022 by the authors. Licensee MDPI, Basel, Switzerland. This article is an open access article distributed under the terms and conditions of the Creative Commons Attribution (CC BY) license (<https://creativecommons.org/licenses/by/4.0/>).

Keywords: bio-desalination; chloride anion; microalgae; kinetic modeling; Saudi Arabia

1. Introduction

Water is regarded as a critical resource for life on the planet's surface. Nowadays, water scarcity is a global issue that many countries are grappling with, particularly those located in dry area belts and highly water-stressed regions [1,2]. Statistics indicate that the amount of water worldwide is estimated to be 1386 billion cubic meters. The predominant proportion (97%) is the salt water in seas and oceans, while fresh water constitutes a small percentage of the total (3%), and if we take into account that 69% of this fresh water is frozen water, this means that the water available for human use is approximately 31% of the total fresh water available; of this, 30% is non-renewable groundwater and only about one percent is renewable water (rivers) [3,4].

The Middle East is currently experiencing a water crisis, with the Kingdom of Saudi Arabia (KSA) and the other Gulf Cooperation Council (GCC) countries (except for Oman) already being classified as water-scarce countries by the United Nations [5].

Overall, water demand in the Kingdom is estimated to be 25.29 billion m³/year (in 2019), but it is predicted to increase to 25.79 billion m³/year by 2025. Therefore, the

KSA has established itself, at the present time, as a global pioneer in the development and application of desalination technologies of saline water, which has now displaced groundwater as the Kingdom's principal source of drinking water.

Arid countries are currently experiencing a water crisis, which is expected to worsen due to agricultural and industrial development resulting from population growth. The rising of water demand causes a variation in prices and intensified competition for its use. Sea water desalination is an inevitable and significant choice for maintaining the water supply in arid and semi-arid regions, especially coastal ones due to their soil, land, and climate characteristics as well as their lack of surface water and fresh underground water supplies [6,7].

The desalination of sea water is now carried out by various methods and technologies around the world, depending on the amount and quality of water needed [7,8]. Due to rising energy costs, conventional desalination systems, such as multiple effect distillation (MED), reverse osmosis (RO), ion exchange (IX), vapor compression distillation (VCD), membrane distillation (MD) electrodialysis (ED), and multistage flash evaporation (MSF), are energy-intensive and, thus, expensive [9–11]. In addition to energy expenses, there are serious issues related to the foregoing desalination systems, including greenhouse gas emissions, the huge release of heat waste, and high brine accumulation in the environment [12]. As a result, there must be a paradigm shift that necessitates new approaches.

Biodesalination is a novel desalination technique based on the absorption (bioaccumulation) and adsorption of salts from saline water by various salt-tolerant living organisms. In comparison to the aforementioned conventional desalination techniques, biological desalination systems consume less energy, have a lower environmental impact, and require less engineering complexity. As a result, they are regarded as a more environmentally friendly for long-term desalination processes [13].

Algae is a common bio-remediated organism that provides high levels of organic removal and pathogen retraction for municipal wastewater treatment [14–16], and it can be employed as a biosorption and bioaccumulation agent for industrial uses [17–22]. Algae are novel and cost-effective biological techniques for the desalination of seawater, and they produce fresh water for a range of applications [23–25]. However, studies related to the use of microalgae for salt removal purposes have limitations. *Scenedismus* sp. is a commonly used freshwater microalgal species with high tolerance to high salinity stress [26,27]. Furthermore, the algae *Scenedismus* sp. can survive in changing environmental conditions due to its high reproduction rate and great vitality [28,29]. In [30], the uptake of NaCl and salt tolerance by microalgae was studied, and it was suggested that bioaccumulation (absorption) and biosorption (adsorption) usually happen in most living organisms. Furthermore, their data revealed that maximal bioaccumulation of salt by algae was achieved after 10 running days under different experimental conditions (different algae species, salinities, nutrient levels, etc.).

The removal mechanisms of salt from seawater or metal from industrial wastewater using microalgae can be explained by two pathways: metabolism-dependent and non-metabolism-dependent. Bioaccumulation is a metabolism-dependent process in which salts are incorporated into algae cells. However, the adsorption is non-metabolism-dependent and is related to the physical bonding or adherence of ions and molecules to the surface of the algae [31].

Microalgal biomass propagated through the water and treated wastewater can be harvested and effectively utilized in different bioproducts, for example, biofuels, bioactive compounds, and pharmaceuticals (antibacterial, antiviral, antitumor/anticancer, antihistamine). In addition, microalgae have been used as health food products for humans, feed for livestock and fish, or as high-value chemicals and pigments [14]. This study aims to evaluate the efficiency of living algal species as a novel and non-conventional approach to the biodesalination of seawater chloride anions. This evaluation was conducted under different biodesalination conditions (seawater concentration, incubation time, light intensity, and CO₂). These conditions were optimized for enhanced seawater biodesalination, and

the quantity of the net algal biomass was taken into consideration. The study's findings can be used to drive the design of a photobioreactor desalination system as well as to support the possibility of recycling algal biomass as a byproduct for multiple beneficial uses.

2. Materials and Methods

2.1. Seawater Sample Collection

Sea water samples were collected from different areas of Tabuk along the Saudi Arabian Red Sea Coast, Figure 1. The sample locations were determined using the Garmin Global Positioning System (GPS) with recent Google map images, as shown in Table 1. The water samples were collected in sterilized plastic bottles and kept for further study. They were transferred to the National Research Center Labs, located in Egypt, for analysis.

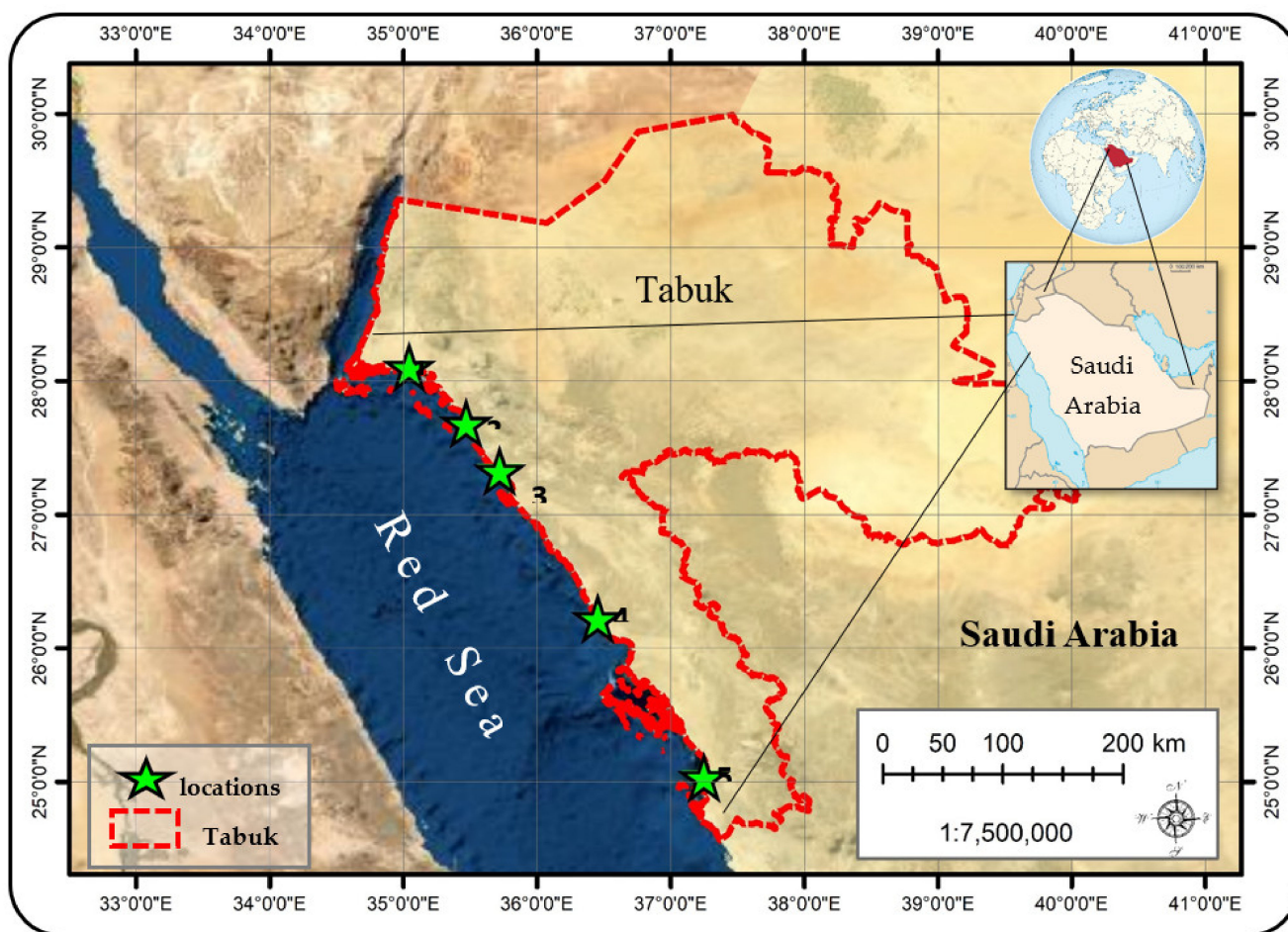


Figure 1. Study Area Map for the five samples collected from Tabuk, Saudi Arabia, Asian Red Sea coast (Using Landsat8 OLI 2022, Path/Row 178/39).

Table 1. Sample location ordination with google map images.

Stand	Location Name	Latitude	Longitude	Google Map Image
1	Gayal	35°02'40.878" E	28°06'21.673" N	
2	Sharma	35°28'19.076" E	27°41'10.930" N	
3	Al-Muwaileh	35°43'20.724" E	27°19'46.699" N	
4	Duba	36°27'22.473" E	26°13'31.834" N	
5	Umluj	37°15'08.167" E	25°02'07.936" N	

2.2. Physical and Chemical Analyses of the Collected Samples

Physical and chemical examinations of water samples were carried out using the procedures outlined by the American Public Health Association [32]. pH was assessed via the pH meter model (Jenway 3505), and electrical conductivity (EC, mS/cm) was assessed via the conductivity meter model (Jenway 4510). The total dissolved solids (TDS) was determined by passing a volume of sample through the Whatman membrane filter (0.45), and a known weight of filtrate was evaporated at 105 °C. Total hardness (Calcium and magnesium) was determined using a complexometric technique via direct titration with EDTA solution. Chlorides were assayed using direct titration with AgNO₃ solution. Sulfates were assessed via turbidimetric techniques. Nitrites were detected using a colorimetric procedure by the formation of a reddish purple azo-dye. The nitrate concentration was determined with the sodium salicylate method. The total Phosphorous concentration was determined calorimetrically using the stannous chloride method.

All colorimetric measurements were performed using a UV *Vis* spectrophotometer Agilent Cary series. Sodium and potassium measurements were performed using 240FS AA-Flame Atomic Absorption.

2.3. Algae Species Isolation and Algal Bioassay Procedures for Biodesalination

Three microalgal species, *S. arcuatusa*, *C. vulgaris*, and *Sp. maxima*, as shown in Figure 2, were collected from Nile water. The three algal species were identified using the main references used for phytoplankton identification [33] and were isolated according to [34,35]. The selection of these algae was due to their salt tolerance characteristics [36–38]. They were cultivated using BG-11 medium [39]. An algal bioassay procedure was used to assess the algal bioaccumulation and growth response against the seawater strength. A composite seawater sample was mixed from the different locations and tested at various concentrations, namely, 100, 75, 50, and 25%. BG-11 medium was added to promote algal growth. Isolated algae in the logarithmic growth phase were inoculated in 250 mL samples of seawater and then feeded by algal nutrients from the BG-11 culture medium at 24 ± 2 °C under continuous fluorescent light (2.800 ft C foot candle) and shaken once per day to prevent algal cell clumping. A linear relationship ($R^2 = 0.999$) between the weight of dry algae and the value of OD 665 (optical density of 665 nm, which was the maximum absorption wavelength) for the cultivated fresh algae. Based on this linear relationship, the dry algae weight equivalent to fresh algae could be sampled [40]. The salt concentrations were detected at different time intervals throughout the incubation period.

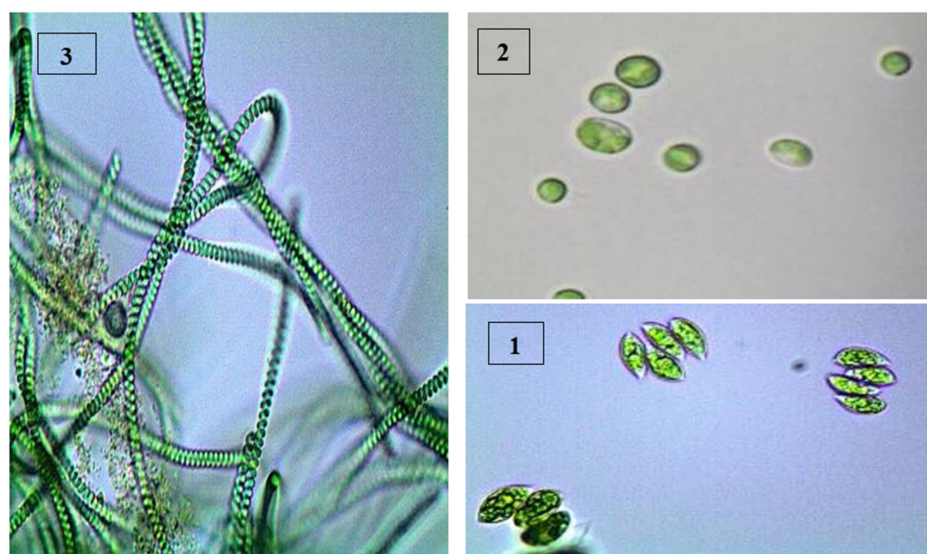


Figure 2. Microscopic photographs (40× magnification) of algal species used in the biodesalination process: (1) *S. arcuatusa*; (2) *C. vulgaris*; and (3) *Sp. Maxima*.

2.4. Biodesalination under High Radiation Light Intensity and CO₂ Supply

The bioassay procedures were modified by subjecting the algal culture in the biodesalination system to a high radiation light intensity and CO₂ supply to accelerate algal growth and increase the salt bioaccumulation rate. Thus, this experiment was conducted under a light source of photosynthetic active radiation (PAR; 400 to 700 nm) to achieve intensities of 100–2000 $\mu\text{mol photons per m}^2 \text{ s}^{-1}$ of PAR with a Source of air and CO₂ pump for gas mixing (~5% CO₂ of enriched air) (see Figure 3).



Figure 3. Biodesalination experimental system: (A) the system under control conditions, (B) the system under high light intensity and CO₂ conditions.

2.5. Desalination Rate Assessment of Chlorides

The rate of seawater desalination determined in the bioassay test was evaluated by measuring TDS. Conductivity was used as a surrogate for TDS, because it can be measured easily and quickly with a conductivity meter, as opposed to TDS measurement, which typically involves filtration, drying, and heating steps. TDS_i indicates the initial conductivity of seawater before the addition of algae. The algae solution was centrifuged at 10,000 rpm for 6 min at the end of each desalination test, and the supernatant was filtered through an 0.45 μm filter and analyzed for conductivity (TDS_f). The algae residue was dried at 60 °C, and the weight difference was detected to assay the net dry algal mass (*m*). The removal efficiency (desalination rate and removal rate of NaCl) and the bioaccumulation capacity of the chloride anion were determined by measurement of the initial (NaCl_i) and final (NaCl_f) chloride anion concentrations using direct titration against AgNO₃ [32]. This was done using methods Equations (1)–(3):

$$\text{Desalination rate (\%)} = (1 - \text{DS}_f / \text{TDS}_i) \times 100 \quad (1)$$

$$\text{Removal rate of NaCl (\%)} = (1 - \text{NaCl}_f / \text{NaCl}_i) \times 100 \quad (2)$$

$$\text{Bioaccumulation capacity of NaCl} = (\text{NaCl}_i - \text{NaCl}_f) / m \quad (3)$$

2.6. Application of Kinetic Modeling

In order to calculate daily bioaccumulation and examine the best fitting **kinetic model** for salt bioaccumulation, two kinetic models, including the pseudo-first order [41], and pseudo-second order equations [42], were applied according to the following two equations:

- **Pseudo First-Order Equation:**

$$\log(Q_e - Q_t) = \log Q_e - \frac{k_1 t}{2.303} \quad (4)$$

where k_1 (1/day) is the rate constant of a pseudo first-order equation, and Q_e (mg/g) and Q_t (mg/g) are the concentrations of bioaccumulated chlorides in the living algal cell at equilibrium and at time t (day), respectively. A straight line of $\ln(Q_e - Q_t)$ versus t suggests that this kinetic model is applicable to the data.

- **Pseudo Second-Order Equation:**

$$\frac{t}{Q_t} = \frac{t}{k_2 Q_e^2} + \frac{t}{Q_e} \quad (5)$$

where k_2 (mg/g day) is the rate constant of a pseudo-second order equation, and Q_e (mg/g) is the concentrations of accumulated salts at equilibrium.

2.7. Characterization of Dried Algal Biomass

At the end of the biodesalination experiments, the net algal biomass was collected by filtration through a Whatman membrane filter with a pore size of 0.45 μm . The biomass was washed carefully several times with distilled water to remove any remaining salts from their cells. Then, the biomass was refiltered. The washed biomass was freeze-dried using a Christ alpha 1–2 LD freeze dryer and then crushed and mixed gently with a mortar and then characterized by Energy dispersive X-ray microanalysis (EDX) and Scanning Electron microscopy (SEM).

3. Results and Discussion

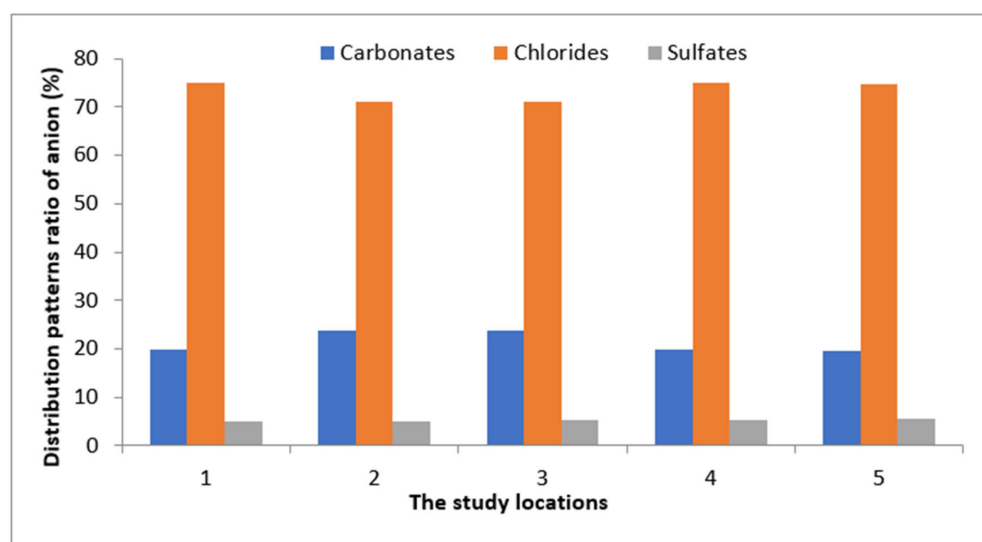
3.1. Physical and Chemical Characterization of the Collected Samples

A water quality analysis was conducted to obtain quantitative and qualitative descriptions of the chemical and physical characteristics. The seawater in the different study areas was characterized to determine the variation in water salinity among them, and the distribution pattern of the ratios and kinds of anions within the total dissolved salts (TDS) were determined. The results obtained for the physico-chemical parameters of the different locations are presented in Table 2. All turbidity values were less than 1.0 NTU. The TDS in seawater samples fluctuated between 37,730 and 40,810 mg/L. The total hardness (as CO_3^{2-}), chloride (as Cl^-) and sulfate (as SO_4^{2-}) concentrations were in the ranges of 7415–9677, 28,245–29,032, and 2070–2100 mg/L, respectively. All of these anions (CO_3^{2-} , Cl^- , and SO_4^{2-}) represent the major dissolved anion salts in seawater samples [43–46].

Figure 4 shows the distribution pattern ratio for the major anion salts relative to the total dissolved salts in the study areas. Representative data reveal that the anion salts can be arranged in descending order among the total dissolved salts as follows: Chlorides > carbonates > sulfates. The above data indicate that there are no meaningful differences between the different locations in terms of physicochemical values, and chloride salt is the major anion salt in the total dissolved salts. These findings are in accordance with data presented by [47–50]. Thus, the chloride anion salt was used in this study as the evaluated parameter to determine the biodesalination efficiency of algae.

Table 2. Physico-chemical analysis at the different locations.

Parameters	Units	Results				
		1	2	3	4	5
pH		8.6	8.52	8.7	8.5	8.61
Turbidity	NTU	0.56	0.49	0.2	0.74	0.26
Electrical Conductivity (EC)	m mhos/cm	57.1	56.2	53.9	54.3	58.3
Total Dissolved Solids (TDS)	mg/L	39,970	39,340	37,730	38,010	40,810
Total Hardness (as CO ₃ ²⁻)	mg/L	9475	7835	7415	7501	9677
Calcium Hardness (as CaCO ₃)	mg/L	3000	2500	2500	2500	3000
Magnesium Hardness (as MgCO ₃)	mg/L	6475	5335	4915	5001	6677
Calcium	mg/L	1200	1000	1000	1000	1200
Magnesium	mg/L	1554	1280.4	1179.6	1200.24	1602.48
Chlorides (as Cl ⁻¹)	mg/L	28,425	29,505	28,245	28,505	29,032
Sulfates (as SO ₄ ⁻²)	mg/L	2070	2000	2070	2003	2100
Nitrite	mg NO ₂ /L	0.0	0.0	0.0	0.0	0.0
Nitrate	mg NO ₃ /L	0.01	0.01	0.01	0.01	0.01
Phosphate	mg P/L	0.0	0.0	0.0	0.0	0.0
Sodium	mg/L	13,268	13,059	12,524	12,617	13,547
Potassium	mg/L	1184	1166	1118	1126	1209

**Figure 4.** The distribution pattern showing the ratios of the major anion salts relative to the total dissolved salts at the study areas. (1) Gayal; (2) Sharma, (3) Al-Muwaileh; (4) Duba; (5) Umluj.

3.2. Effect of the Salinity Concentration on the Rate of Chloride Biodesalination

The efficiency of chloride bioaccumulation in the three microalgae species was assessed at different seawater concentrations. Figure 5 reveals that chloride bioaccumulated significantly in the three algal species as the seawater concentration increased. The maximum chloride bioaccumulation yields in *C. vulgaris*, *Sp. Maxima*, and *S. arcuatusa* sp. were 260, 190, and 150 mg/g fresh weight, respectively.

This result had a positive impact on the seawater quality. TDS removal (Figure 6) ranged from 24.2% (9500 mg/L TDS) to 41.5% (33,375 mg/L TDS) in seawater inoculated by *Sp. maxima* culture, but this removal took a long time (33 days), while *C. vulgaris* achieved about 39.1% TDS removal after only 22 days at a TDS concentration of 17,080 mg/L, thereby increasing the chloride concentration. Interestingly, a clear correlation between salt tolerance and chloride removal was observed by [36] for the case of *C. vulgaris*. Additionally, the TDS reduction values caused by *C. vulgaris* exhibited a positive correlation with the increase in chloride concentration. In [51], it was shown that two species of microalgae,

Nannochloropsis culate and *Dunaliella tertiolecta*, have the ability to decrease the concentration of TDS.

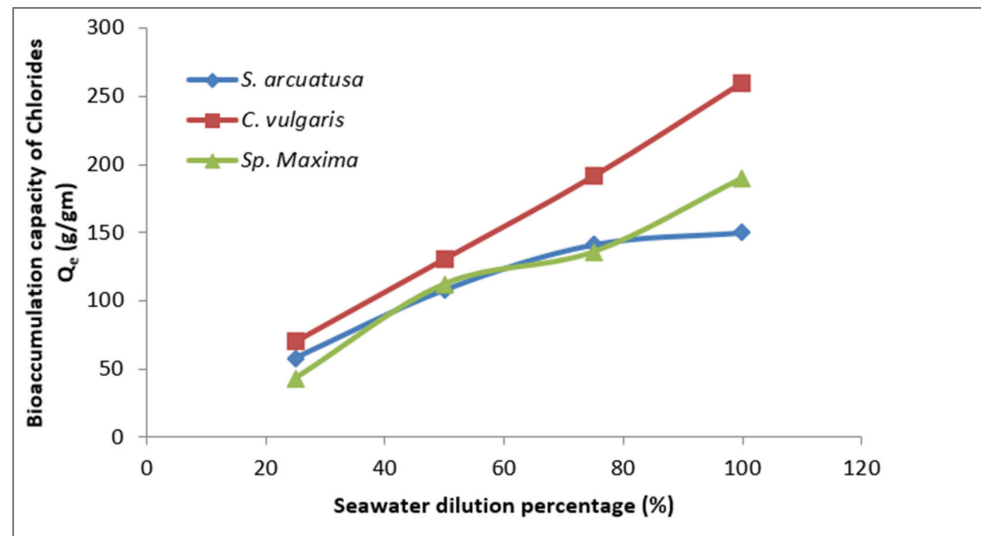


Figure 5. The bioaccumulation capacity of chloride anions (Q_e) at different seawater concentrations.

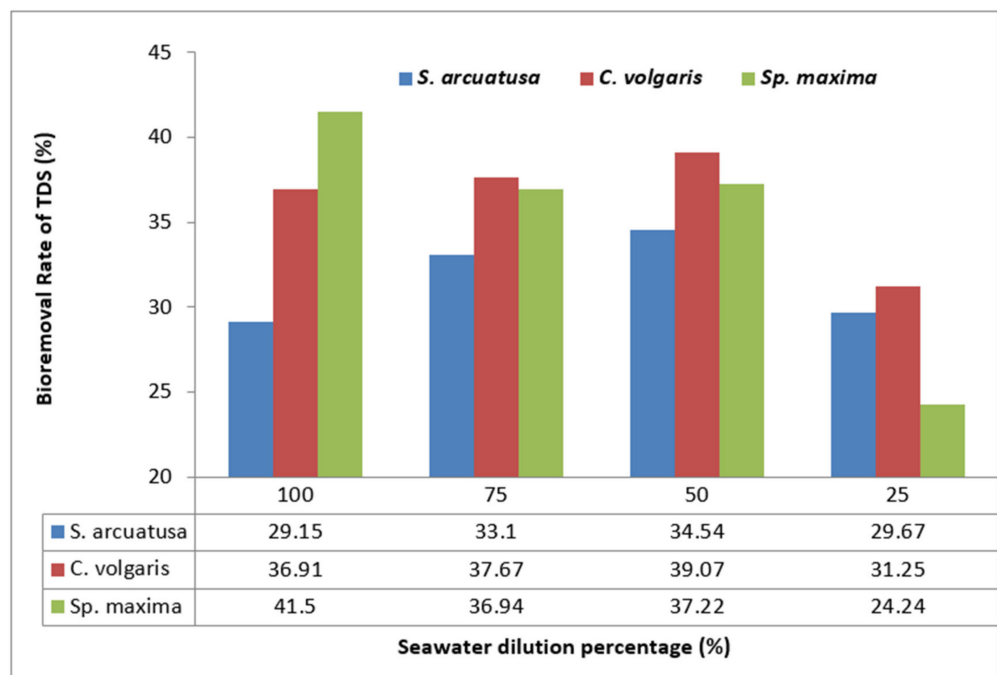


Figure 6. The bioremoval of TDS at different seawater concentrations.

3.3. Effect of the Incubation Period on the Rate of Biodesalination

The effects of the incubation period on biodesalination are shown in Figure 7. It can be seen clearly that the three microalgae exhibited steady increases in the chloride bioaccumulation rate throughout the incubation period until the sixth day with both *S. arcuatusa* and *Sp. Maxima*, and until the eighth day with *C. vulgaris*. The bioaccumulation capacities at these points were 95.9, 74.4, and 64.5 mg/g fresh weight for *C. vulgaris*, *S. arcuatusa*, and *Sp. maxima*, respectively.

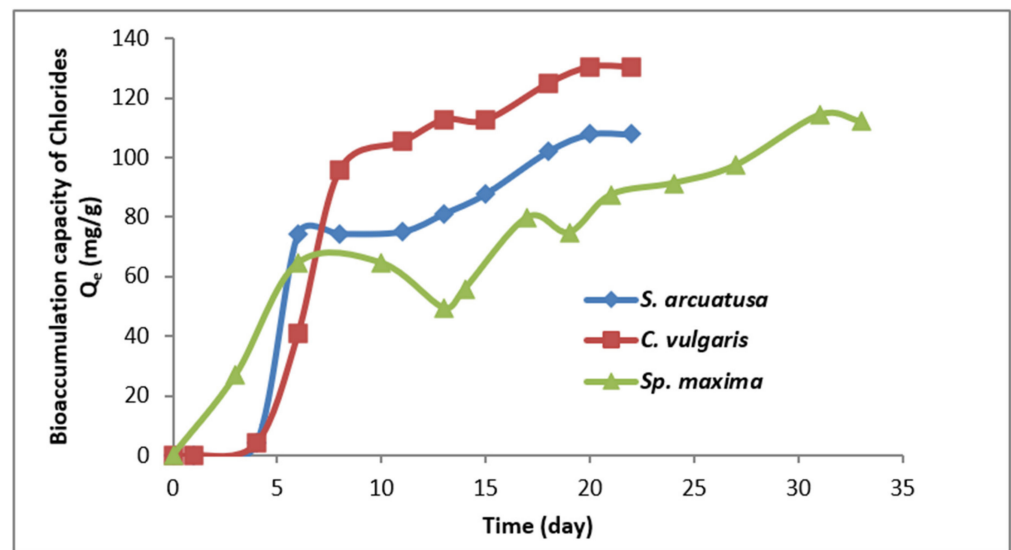


Figure 7. The bioaccumulation of chloride anions by algal species during the incubation period.

The study performed in [52] showed that the bioaccumulation equilibrium achieved by algae ranged from 3.58 to 7.68 per day. After these points, the bioaccumulation rate took longer, and there was no significant change in the bioaccumulation rate compared with the first stage. *C. vulgaris* showed a better bioaccumulation performance than *S. arcuatusa* and *Sp. maxima*. Additionally, *S. arcuatusa*, and *C. vulgaris* showed shorter incubation periods (22 days) than *Sp. maxima* (33 days). At the end of the incubation periods of the three algal species, the total chloride removal proportions were 39.7%, 39.2%, and 32.4% for *Sp. maxima*, *C. vulgaris*, and *S. arcuatusa*, respectively, Figure 8. The maximal bio-accumulation capacity at the end of the incubation period reached 130.5, 114.2, and 107.8 mg/g fresh weight, respectively. In comparison, a study performed by [30] confirmed that full absorption was reached within a relatively short time period, but the removal of salts (only 10%) reached by absorption was not obvious, since over 39% of chloride removal was achieved by bioaccumulation, but this occurred across a longer time frame.

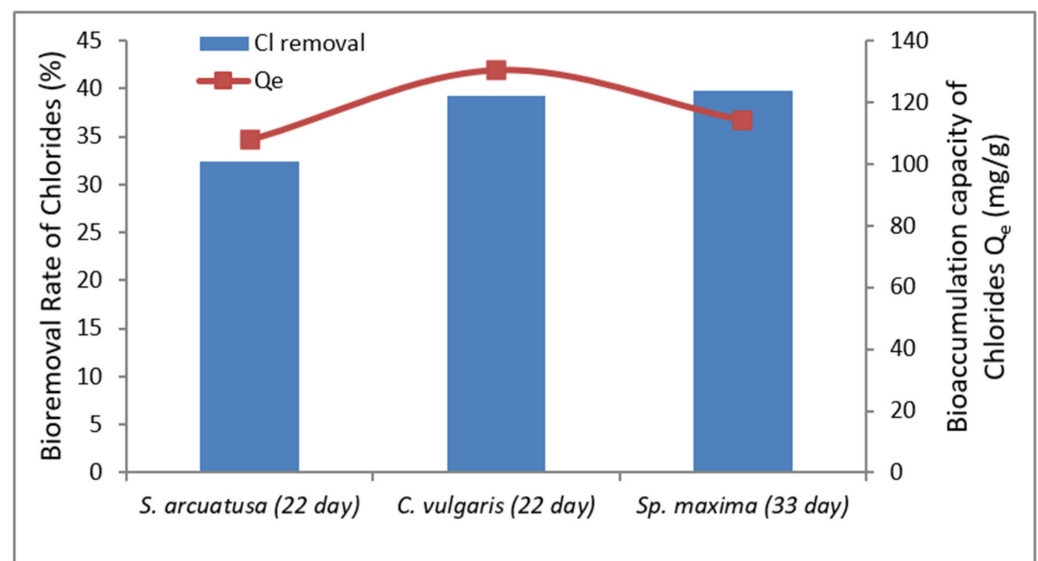


Figure 8. The maximum bioaccumulation capacity and bioremoval rate of chloride anions by the algal species.

3.4. Effect of High Light Radiation Intensity and CO₂ Supply on the Rate of Biodesalination

In order to enhance the bioaccumulation performance of the algae, a new growth condition was applied to the cultured algae in seawater. Since high light radiation of 2000 $\mu\text{mol photons per m}^2 \text{ s}^{-1}$ of PARm was emitted, air and CO₂ were pumped with a gas mixing ratio (~5% CO₂ of enriched air). These conditions were applied at a temperature of 32 °C. These conditions were applied to enhance algal growth. *S. arcuatusa* and *C. vulgaris* flourished under these conditions, but *Sp. maxima* failed to grow. Thus, the data illustrated in Figures 9–11 represent the effects of these conditions on the bioaccumulation efficiency of the two algal species *S. arcuatusa* and *C. vulgaris*.

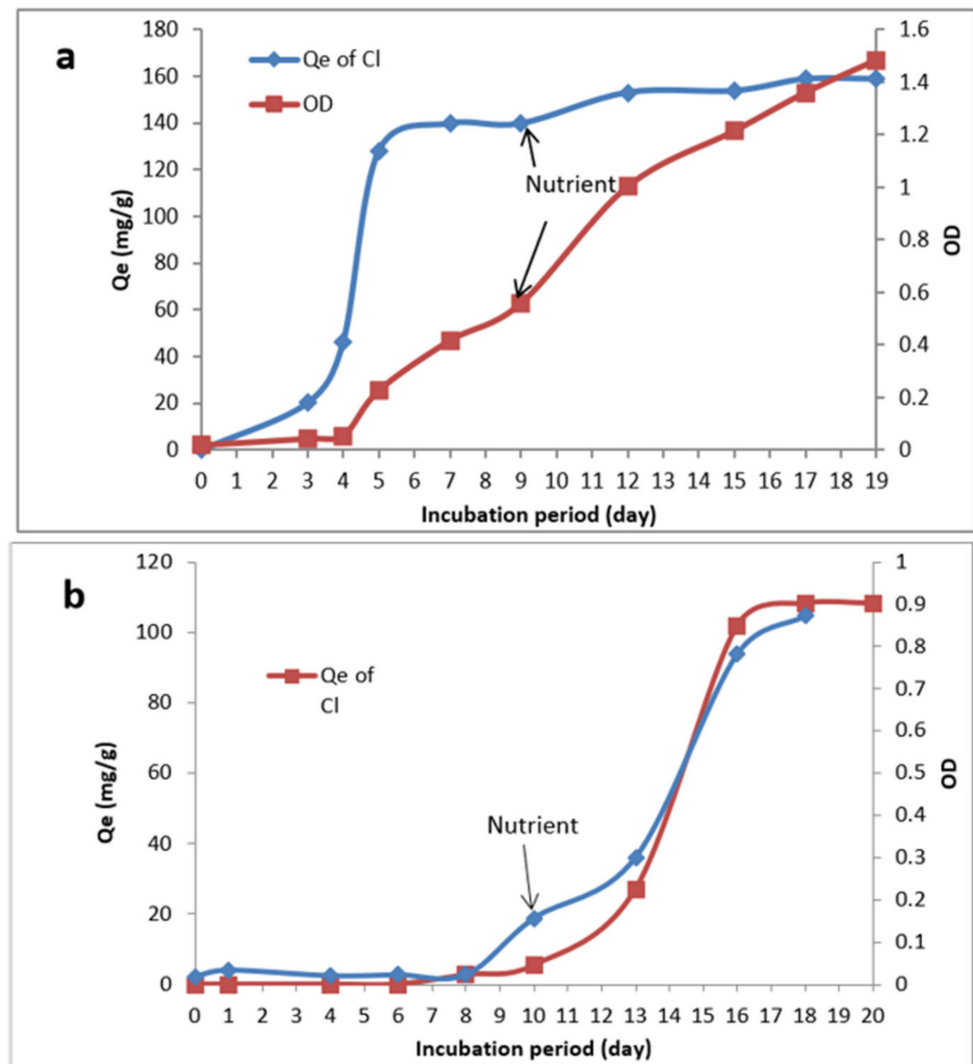


Figure 9. Relationship between the Chloride bioaccumulation capacity (Q_e) and the growth response (OD) in (a) *S. arcuatusa* and (b) *C. vulgaris*.

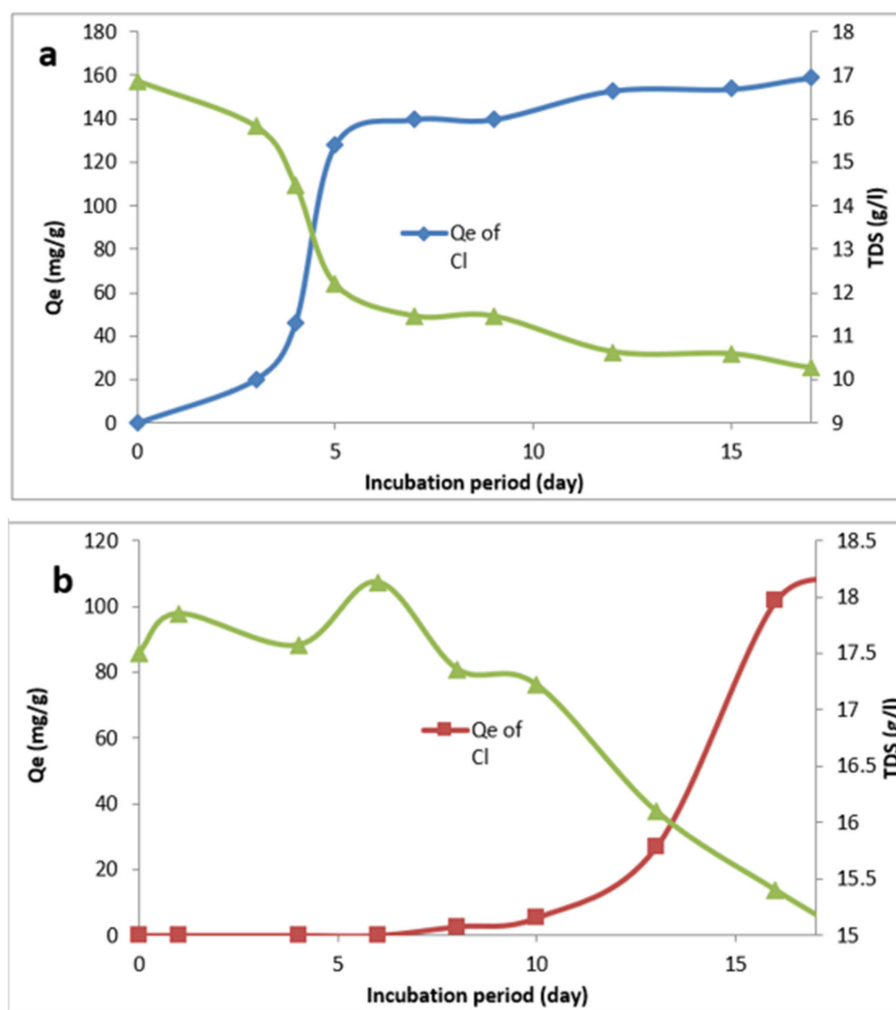


Figure 10. Relationship between the chloride bioaccumulation capacity (Q_e) and TDS in (a) *S. arcuata* and (b) *C. vulgaris*.

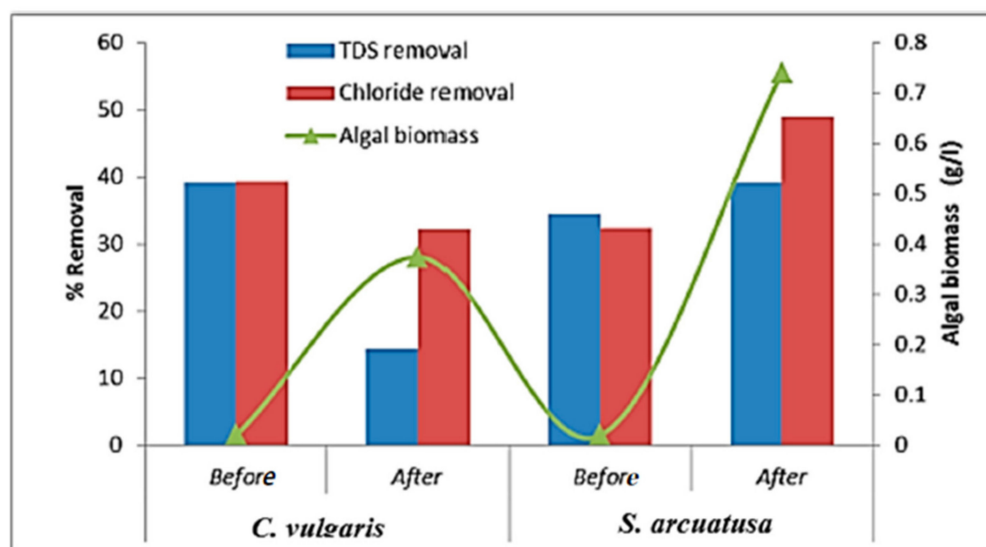


Figure 11. The removal efficiency for TDS and chloride and the net algal biomass in *S. arcuata* and *C. vulgaris* before and after being subjected to new conditions.

The data in Figure 9 show differences in the growth response in the two algal strains. Furthermore, an obvious positive correlation was exhibited between the growth response and the bioaccumulation capacity, where sudden exponential chloride accumulation appeared from the third day until the fifth day. This sudden accumulation behavior was related to the sudden growth response in the same bioaccumulation period. The bioaccumulation reached equilibrium after the fifth day. At the same time, the algal growth continued to undergo exponential growth.

On the ninth day, extra nitrogen and phosphorous were added. This nutrient addition led to more chloride accumulation (increase by 8.7%) and exponential algal growth (increase by 44.3%) until the 12th day. After that the bioaccumulation returned to equilibrium, and the exponential algal growth decreased.

As compared to *S. arcuatusa*, *C. vulgaris* exhibited an excellent correlation between chloride bioaccumulation and the algal growth response, but this correlation was accompanied by weak efficiency until the 10th day. After the nutrient addition, on the 10th day, 94.7% and 80% increases in chloride bioaccumulation and algal growth were exhibited, respectively. On the other hand, Figure 10 shows that an obvious inverse correlation between TDS and the bioaccumulation capacity of chloride by *S. arcuatusa*. This correlation was exhibited in the responses of the two variables. This proves the presence of a strong correlation. This inverse correlation and good consistency were also achieved in *C. vulgaris*, but not to the same degree, due to the weak efficiency.

Figure 11 shows the differences in the removal efficiency of chloride and TDS before and after addressing the new bioaccumulation conditions. However, these conditions had a negative effect on the performance of *C. vulgaris* for TDS removal, where an obvious removal efficiency decline occurred for TDS (from 39.07% to 14.4%) and chloride (from 39.24 to 31.13), but the net algal biomass produced was enhanced (from 0.02 to 0.374 g/L). On the contrary, a positive effect on removal efficiency was achieved under these conditions by *S. arcuatusa*, where TDS and chloride removal were enhanced (from 34.54 to 39.09% and from 32.42 to 48.93%), and an obvious net algal biomass production enhancement occurred (from 0.02 to 0.740 g/L). Different studies have reported that high growth acceleration due to a high light intensity and CO₂ supply promote a high bioaccumulation efficiency. According to [53], algae-based bioremediation produces more biomass due to its strong potential to bioaccumulate, degrade, or detoxify xenobiotics and contaminants. In [54], it was discovered that greater light intensities have a considerable effect on algal biomass production, and the culture system swiftly transitions from a mixotrophic-dominated mode to a photoautotrophic-dominated mode. The addition of a larger CO₂ injection rate would result in a higher degree of carbon fixation, and the impacts of light and CO₂ would accelerate the process of bioaccumulation. In [31], it was stated that the major component for algal productivity is photosynthetic active radiation (PAR) pulsed from the light source, with the best range of photon flux being between 30 and 400 mol/m² s. Increasing the available amount of CO₂ can boost the algal biomass output.

Furthermore, it has been demonstrated that algae are able to complete their life cycles in a wide range of salinity levels with differences existing even within species. The application of these algae and microorganisms or their combination can be an effective way to undergo desalting or reduce the water salinity [23,25,55].

3.5. Kinetic Modeling for Biodesalination

3.5.1. Kinetics of Chloride Bioaccumulation by Algae under Control Conditions

Under the control conditions, the three algal species bioaccumulated the chloride anions along different incubation period time intervals. In order to evaluate the daily bio-accumulation capacity during the incubation period, two kinetic models were applied. The pseudo-first and pseudo-second order kinetic models are shown in Figure 12.

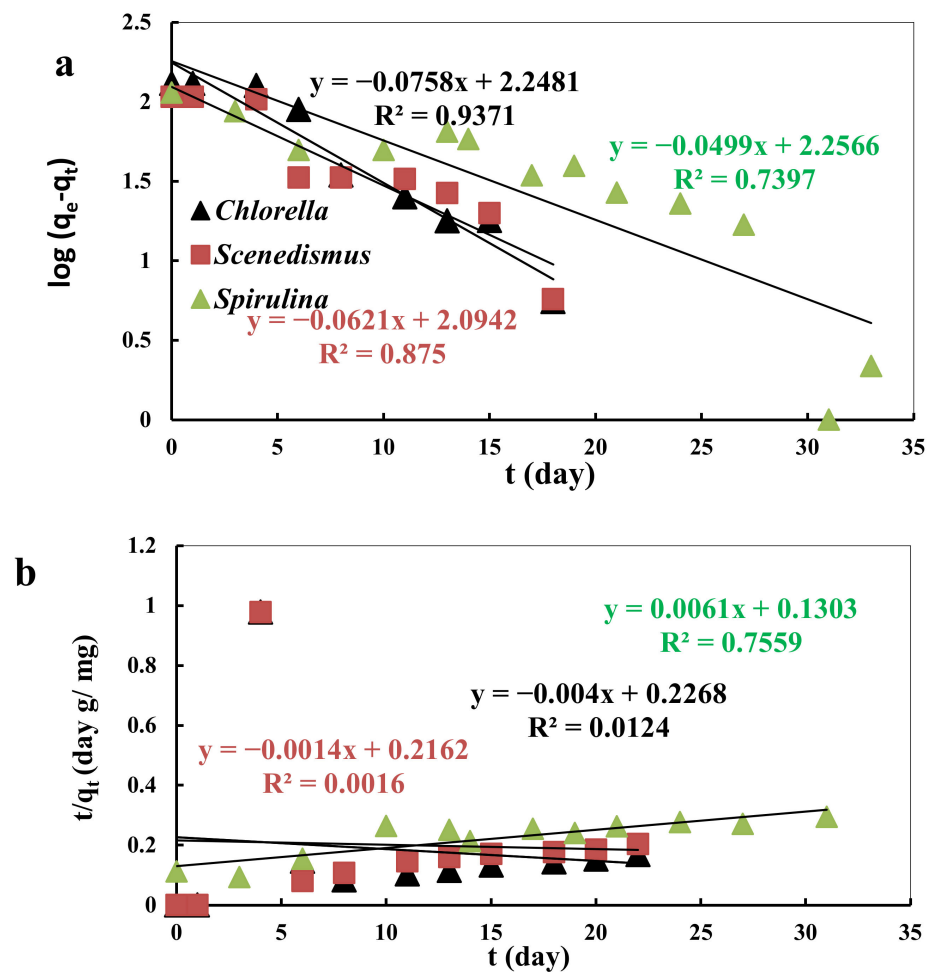


Figure 12. Kinetic plots showing (a) pseudo first order and (b) pseudo second order models of the three algal species under control conditions.

Only the experimental data of *C. vulgaris* were fitted to the pseudo-first-order model, where the obtained R^2 value for chloride bioaccumulation was more than 0.93, but the calculated (Q_e) value (177 mg/g/day) was closer to the experimental value (130) than the value for the second order kinetic model (250), which had an R^2 value of less than 0.9. However, the obtained R^2 values from the pseudo-first-order model for *S. arcuatusa* and *Sp. maxima* were 0.875 and 0.739, respectively. These values do not fit with the pseudo-first-order model, but the experimental Q_e value of *S. arcuatusa* (124 mg/g/day) was closer to the calculated (Q_e) value (107), while the experimental Q_e value of the pseudo-first-order model for *Sp. maxima* (180 mg/g/day) was not closer to the calculated (Q_e) value (114). In [52], it was confirmed that the initial salt uptake by algae followed pseudo first-order kinetics.

All pseudo-second order kinetic models for *C. vulgaris*, *S. arcuatusa*, and *Sp. maxima* were not fitted due to having R^2 values of less than 0.9 and experimental and calculated Q_e values that did not match those shown in Table 3, except for the case of *Sp. maxima*, where the calculated (Q_e) value (114) was closer to calculated value (133.3), suggesting that the bioaccumulation of chloride anions by *C. vulgaris* only fits well to the pseudo-first order model. Daily bioaccumulation rates were 177, 124, and 133.3 mg/g/day for *C. vulgaris*, *S. arcuatusa*, and *Sp. maxima*, respectively.

Table 3. Kinetic parameters of chloride bioaccumulation by the three algal species.

	Pseudo-First Order				Pseudo-Second Order			
	Q _e (mg/g) (Cal)	Q _e (mg/g) (Exp.)	K ₁ (min ⁻¹)	R ²	Q _e (mg/g) (cal.)	Q _e (mg/g) (exp.)	K ₂ (g/mg/min)	R ²
<i>C. vulgaris</i>	177	130.5	0.174	0.937	250	130.5	0.00007	0.0124
<i>S. arcuatusa</i>	124.2	107.8	0.143	0.875	714.3	107.8	9.065	0.0016
<i>Sp. maxima</i>	180.55	114.23	0.115	0.739	133.3	114.23	0.00069	0.7559

3.5.2. Kinetic Modeling under High Light Intensity and CO₂ Supply

Under high light intensity and CO₂ supply, the algal species exhibited different bioaccumulation kinetic behaviors. Figure 13 show the pseudo first and second order kinetics after the algal species had been subjected to these conditions. The illustrated data prove that the experimental data from *S. arcuatusa* alone could be fitted to the pseudo-first-order model, where the R² value obtained for chloride bioaccumulation was more than 0.95, and the calculated (Q_e) value (158 mg/g/day) was slightly closer to the experimental (Q_e) value (210). However, for *C. vulgaris*, neither the R² value nor the experimental (Q_e) values were fitted, because their data did not match the pseudo-first-order equation. In addition, the (Q_e) value of *C. vulgaris* was reduced under these conditions from 177 into 107 mg/g/day, but for *S. arcuatusa*, there was a noticeable enhancement in Q_e from 124 to 210 mg/g/day.

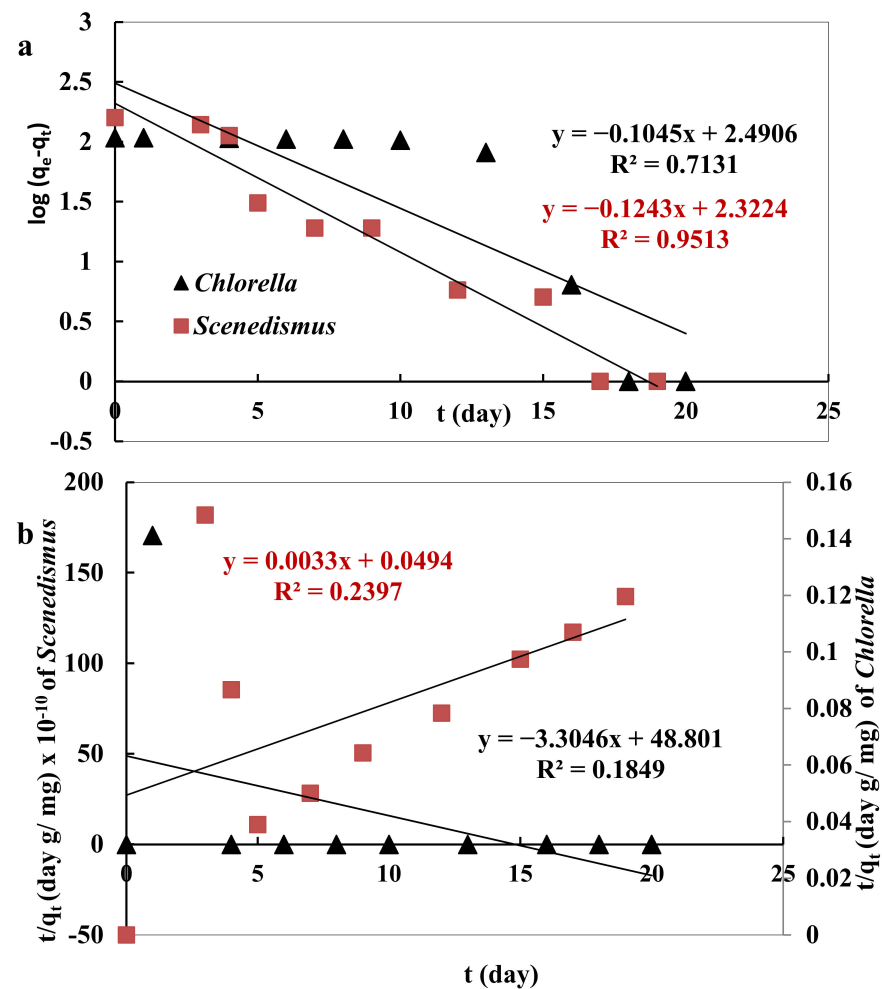


Figure 13. Kinetic plots showing (a) pseudo first order and (b) pseudo second order models of the algal species under high light intensity and CO₂ supply.

In an investigation of two types of halophytic microalgae by [52], it was found that the initial salt uptake followed pseudo first order kinetics, where the rate constant ranged from -3.58 to -7.68 per day, reaching up to 30% in a single cycle.

3.6. The Effect of Sea Water on Algal Morphological Changes

Some deformation in algal species morphology occurred when they were subjected to seawater conditions. These deformations are shown in Figure 14, representing *S. arcuatusa* algal cells before and after exposure to high salinity conditions. The most noted deformation features were the shrinkage in cell size and separation of the quadrate jointed cells into scattered solitary cells. Many morphological changes due to water salinity stress have been examined in different studies for algal species such as *Chlamydomonas* [56], *Gracilatia* sp. *venucosa*, *Gmcilatia* sp. and *Ptemcladia capillacea* [57], and *Kirchneriella* sp. [58].

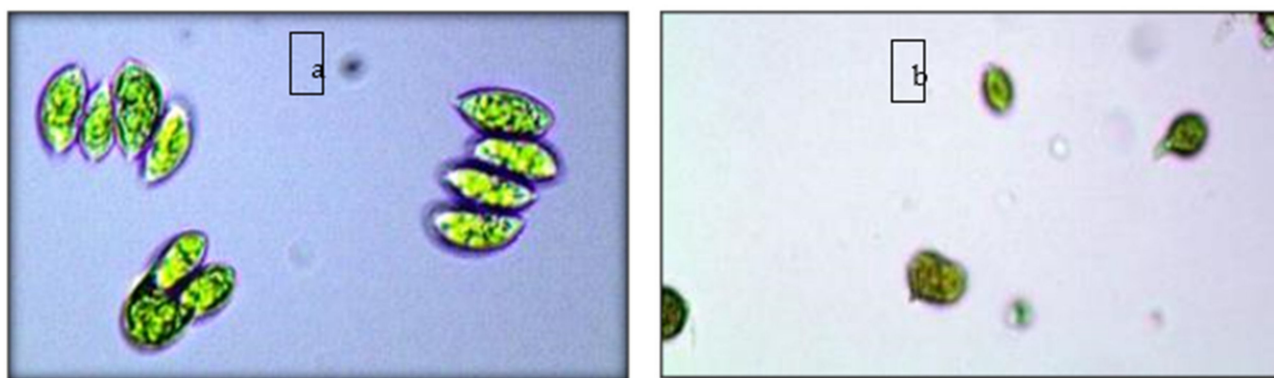


Figure 14. Microscopic photographs (40× magnification) of *S. arcuatusa* (a) before and (b) after exposure to high salinity conditions.

3.7. Characterization of Dried Algal Biomass

3.7.1. Energy Dispersive X-ray Microanalysis (EDX)

The elemental composition of the freeze-dried algal biomass algae was characterized by EDX microanalysis. This technique can help to identify the presence of various elements inside the biomass in order to determine the major elements entrapped in microalgae during the bioaccumulation.

As shown in Table 4, of algal biomass materials, C and O were the most abundant components due to CO_2 sequestration during photosynthesis [31]. They were notable increase in Na^+ and K^+ after biodesalination. In contrast, the Mg^{2+} and Ca^{2+} concentrations decreased after biodesalination. This may be attributed to the replacement of Ca^{2+} and Mg^{2+} with Na^+ and K^+ through the algal cells. This finding was confirmed by [36,59].

Table 4. Energy dispersive X-ray microanalysis (EDX) for algal biomass before and after bioaccumulation.

Element	Weight (%)	
	Before	After
C	66.19	66.35
O	26.59	26.65
Na^+	0.94	1.15
K^+	2.38	3.32
Mg^{2+}	1.53	0.49
Ca^{2+}	2.35	2.02

3.7.2. Scanning Electron Microscopy (SEM) Analysis of Dried Algal Biomass

The dried algal biomass was investigated by SEM (Figure 15) before and after biodesalination to provide more information about the change in topography structure of the

algae due to the desalination conditions. It was observed that white batches of salt were accumulated and embedded into the algal biomass. This observation proves the occurrence of the accumulation of salt inside the algal cells.

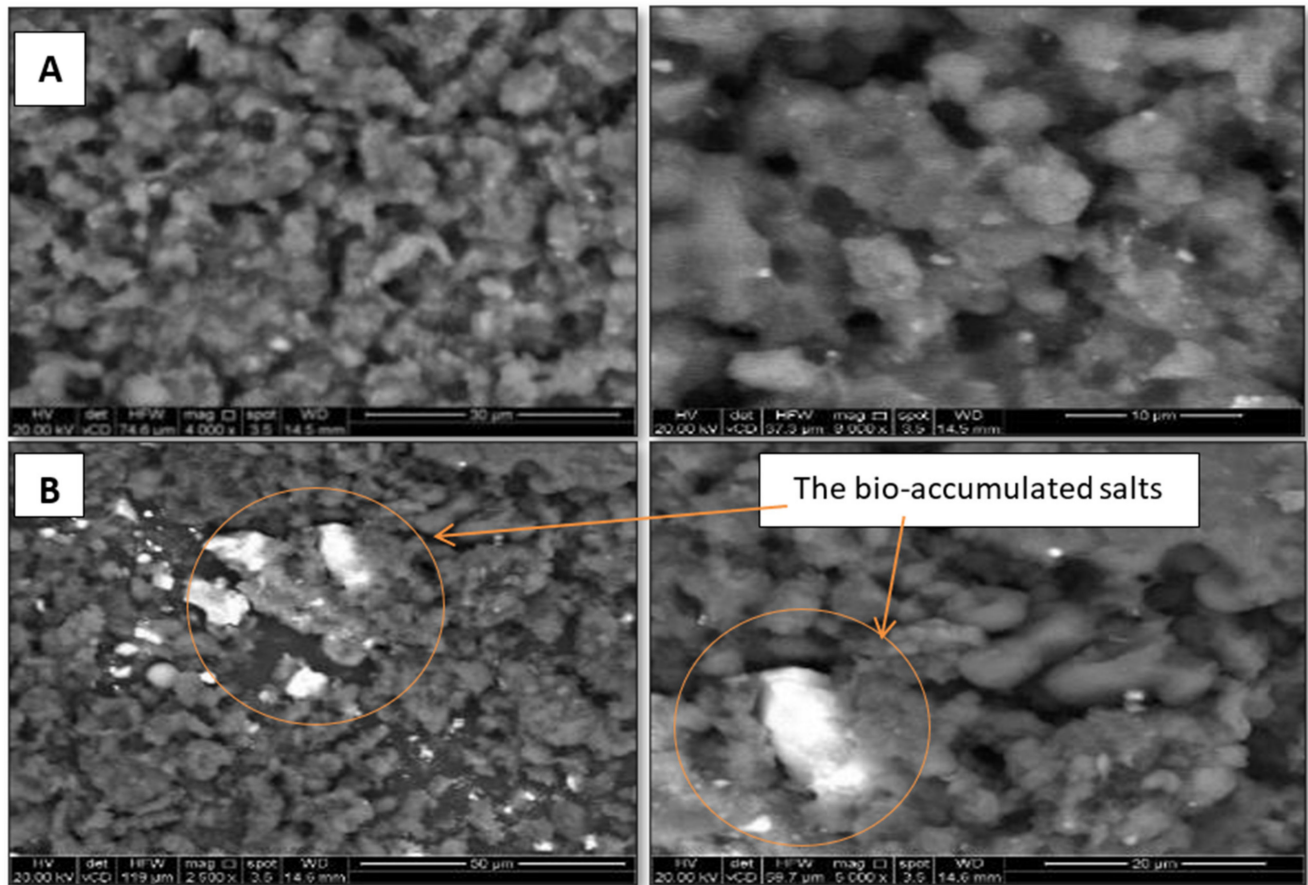


Figure 15. SEM micrographs for dried algal biomass (A) before and (B) after bio-desalination.

4. Conclusions and Recommendations

In this work, three algal species, *S. arcuatusa*, *C. vulgaris*, and *Sp. Maxima*, were investigated under different operating conditions to explore their biological desalination efficiencies. It was revealed that under a high light intensity and CO₂ supply, *S. arcuatusa* enhanced chloride removal from 32.42 to 48.93%, the daily bio-accumulation capacity (Q_e) according to the kinetic models was enhanced from 124 to 210 mg/g/day, and the net biomass production was enhanced from 0.02 to 0.740 g/L. The results of the EDX analysis suggest that the bioaccumulation mechanism mainly depends on the replacement of Ca²⁺ and Mg²⁺ with Na⁺ and K⁺ through algal cells. The above findings suggest that algae show promise for use in energy-efficient techniques as an alternative ecofriendly desalination technology. It is recommended that the net biomass of desalination be reused to produce high-value byproducts, such as pharmaceuticals and bioactive compounds, biofuels, and chemicals. The above data suggest the need for further work in this area. This work will be the precursor for upscaling photobioreactor systems for seawater desalination and algal biomass production to allow algae to be used for the production of valuable economic products, such as biofuels, pharmaceuticals, bioactive compounds, high-value products, and chemicals. Ultimately, the current and future work related to this study could aid in the development of the NEOM region in the KSA.

Author Contributions: Data curation, M.O.I.G., O.B., A.A., M.M.A. and M.M.I.H.; Formal analysis, M.M.I.H.; Funding acquisition, M.O.I.G.; Investigation, A.A. and M.M.A.; Methodology, M.O.I.G.,

M.M.A. and M.M.I.H.; Project administration, M.O.I.G.; Resources, O.B.; Software, M.M.I.H.; Supervision, M.O.I.G.; Visualization, O.B.; Writing—review & editing, M.O.I.G. and M.M.I.H. All authors have read and agreed to the published version of the manuscript.

Funding: This research was funded by The Deputyship for Research & Innovation, Ministry of Education in Saudi Arabia, the project number (0011-1442-S).

Acknowledgments: The authors extend their appreciation to the Deputyship for Research & Innovation, Ministry of Education in Saudi Arabia for funding this research work under project number (0011-1442-S).

Conflicts of Interest: The authors declare no conflict of interest.

References

1. Abdel-Raouf, N.; Al-Homaidan, A.A.; Ibraheem, I.B.M. Microalgae and wastewater treatment. *Saudi J. Biol. Sci.* **2012**, *19*, 257–275. [[CrossRef](#)] [[PubMed](#)]
2. Panhwar, M.Y.; Panhwar, S.; Keerio, H.A.; Khokhar, N.H.; Shah, S.A.; Pathan, N. Water quality analysis of old and new Phuleli Canal for irrigation purpose in the vicinity of Hyderabad, Pakistan. *Water Pract. Technol.* **2022**, *17*, 529–536. [[CrossRef](#)]
3. Bigas, H. *The Global Water Crisis: Addressing an Urgent Security Issue*; United Nations University—Institute for Water, Environment and Health: Hamilton, ON, Canada, 2012; 176p.
4. Chen, C.; Jiang, Y.; Ye, Z.; Yang, Y.; Hou, L. Sustainably integrating desalination with solar power to overcome future freshwater scarcity in China. *Glob. Energy Interconnect.* **2019**, *2*, 98–113. [[CrossRef](#)]
5. Samad, N.A.; Bruno, V.L. The urgency of preserving water resources. *Environ. News* **2013**, *21*, 3–6.
6. McGinn, P.J.; Dickinson, K.E.; Park, K.C.; Whitney, C.G.; MacQuarrie, S.P.; Black, F.J.; Frigon, J.-C.; Guiot, S.R.; O’Leary, S.J. Assessment of the bioenergy and bioremediation potentials of the microalga *Scenedesmus* sp. AMDD cultivated in municipal wastewater effluent in batch and continuous mode. *Algal Res.* **2012**, *1*, 155–165. [[CrossRef](#)]
7. Pittman, J.K.; Dean, A.P.; Osundeko, O. The potential of sustainable algal biofuel production using wastewater resources. *Bioresour. Technol.* **2011**, *102*, 17–25. [[CrossRef](#)] [[PubMed](#)]
8. Gorjian, S.; Ghobadian, B. Solar desalination: A sustainable solution to water crisis in Iran. *Renew. Sustain. Energy Rev.* **2015**, *48*, 571–584. [[CrossRef](#)]
9. Sehn, P. Fluoride removal with extra low energy reverse osmosis membranes: Three years of large scale field experience in Finland. *Desalination* **2008**, *223*, 73–84. [[CrossRef](#)]
10. Mezher, T.; Fath, H.; Abbas, Z.; Khaled, A. Techno-economic assessment and environmental impacts of desalination technologies. *Desalination* **2011**, *266*, 263–273. [[CrossRef](#)]
11. Al-Odwani, A.; El-Sayed, E.E.F.; Al-Tabtabaei, M.; Safar, M. Corrosion resistance and performance of copper–nickel and titanium alloys in MSF distillation plants. *Desalination* **2006**, *201*, 46–57. [[CrossRef](#)]
12. Ashwaniy, V.R.V.; Perumalsamy, M. Reduction of organic compounds in petro-chemical industry effluent and desalination using *Scenedesmus* abundans algal microbial desalination cell. *J. Environ. Chem. Eng.* **2017**, *5*, 5961–5967. [[CrossRef](#)]
13. Wang, S.; Yang, S.; Jin, X.; Liu, L.; Wu, F. Use of low cost crop biological wastes for the removal of Nitrobenzene from water. *Desalination* **2010**, *264*, 32–36. [[CrossRef](#)]
14. Doma, H.; Moghazy, R.; Mahmoud, R. Environmental factors controlling algal species succession in High Rate Algal Pond. *Egypt. J. Chem.* **2021**, *64*, 729–738. [[CrossRef](#)]
15. El-Kamah, H.M.; Badr, S.A.; Moghazy, R.M. Reuse of Wastewater Treated Effluent by Lagoon for Agriculture and Aquaculture Purposes. *Aust. J. Basic Appl. Sci.* **2011**, *5*, 9–17.
16. El-Kamah, H.M.; Doma, H.S.; Badr, S.; El-Shafai, S.A.; Moghazy, R.M. Removal of fecal coliform from HFBR effluent via stabilization pond as a post treatment. *Res. J. Pharm. Biol. Chem. Sci.* **2016**, *7*, 1897–1905.
17. Moghazy, R.M.; Labena, A.; Husien, S.; Mansor, E.S.; Abdelhamid, A.E. Neoteric approach for efficient eco-friendly dye removal and recovery using algal-polymer biosorbent sheets: Characterization, factorial design, equilibrium and kinetics. *Int. J. Biol. Macromol.* **2020**, *157*, 494–509. [[CrossRef](#)]
18. Moghazy, R.M.; Labena, A.; Husien, S. Eco-friendly complementary biosorption process of methylene blue using micro-sized dried biosorbents of two macro-algal species (*Ulva fasciata* and *Sargassum dentifolium*): Full factorial design, equilibrium, and kinetic studies. *Int. J. Biol. Macromol.* **2019**, *134*, 330–343. [[CrossRef](#)] [[PubMed](#)]
19. Abdelhamid, A.E.; Labena, A.; Mansor, E.S.; Husien, S.; Moghazy, R.M. Highly efficient adsorptive membrane for heavy metal removal based on *Ulva fasciata* biomass. *Biomass Conv. Bioref.* **2021**, *11*, 1–16. [[CrossRef](#)]
20. Moghazy, R.M. Activated biomass of the green microalga *Chlamydomonas variabilis* as an efficient biosorbent to remove methylene blue dye from aqueous solutions. *Water SA* **2019**, *45*, 20–28. [[CrossRef](#)]
21. Abdelhameed, R.M.; Alzahrani, E.; Shaltout, A.A.; Moghazy, R.M. Development of biological macroalgae lignins using copper based metal-organic framework for selective adsorption of cationic dye from mixed dyes. *Int. J. Biol. Macromol.* **2020**, *165*, 2984–2993. [[CrossRef](#)]

22. Badr, S.A.; Ashmawy, A.A.; El-Sherif, I.Y.; Moghazy, R.M. Non-conventional low-cost biosorbents for adsorption and desorption of heavy metals. *Res. J. Pharm. Biol. Chem. Sci.* **2016**, *7*, 3110–3122.
23. Kesaano, M.; Sims, R.C. Algal biofilm based technology for wastewater treatment. *Algal Res.* **2014**, *5*, 231–240. [[CrossRef](#)]
24. Nagy, A.M.; El Nadi, M.H.; Hussein, H.M. Determination of the best water depth in desalination algae ponds. *El Azhar Univ. Fac. Eng. CERM Civ. Eng.* **2019**, *38*, 1.
25. Park, J.; Jin, H.-F.; Lim, B.-R.; Park, K.-Y.; Lee, K. Ammonia removal from anaerobic digestion effluent of livestock waste using green alga *Scenedesmus* sp. *Bioresour. Technol.* **2010**, *101*, 8649–8657. [[CrossRef](#)]
26. Demetriou, G.; Neonaki, C.; Navakoudis, E.; Kotzabasis, K. Salt stress impact on the molecular structure and function of the photosynthetic apparatus—The protective role of polyamines. *Biochim. Biophys. Acta* **2007**, *1767*, 272–280. [[CrossRef](#)]
27. Mohammed, A.A.; Shafea, A.A. Growth and some metabolic activities of *Scenedesmus obliquus* cultivated under different NaCl concentrations. *Biol. Plant.* **1992**, *34*, 423–430. [[CrossRef](#)]
28. Martínez, M.E.; Sánchez, S.; Jiménez, J.M.; El Yousfi, F.; Muñoz, L. Nitrogen and phosphorus removal from urban wastewater by the microalga *Scenedesmus obliquus*. *Bioresour. Technol.* **2000**, *73*, 263–272. [[CrossRef](#)]
29. Lewis, M.A. Use of freshwater plants for phytotoxicity testing: A review. *Environ. Pollut.* **1995**, *87*, 319–336. [[CrossRef](#)]
30. Wei, J.; Gao, L.; Shen, G.; Yang, X.; Li, M. The role of adsorption in microalgae biological desalination: Salt removal from brackish water using *Scenedesmus obliquus*. *Desalination* **2020**, *493*, 114616. [[CrossRef](#)]
31. Moghazy, R.M.; Abdo, S.M.; Mahmoud, R.H. Chapter 7—Algal Biomass as a Promising Tool for CO₂ Sequestration and Wastewater Bioremediation: An Integration of Green Technology for Different Aspects; Elsevier: Amsterdam, The Netherlands, 2022; pp. 149–166.
32. APHA. *Standard Methods for the Examination of Water and Wastewater*; APHA: Washington, DC, USA, 2017.
33. Streble, H.; Krauter, D. Das Leben im Wassertropfen: Mikroflora und Mikrofauna des Süßwassers. In *Ein Bestimmungsbuch*; Franckh-Kosmos Verlags-GmbH & Co.: Stuttgart, Germany, 2006.
34. Baker, P.D.; Fabbro, L. *A Guide to the Identification of Common Blue-Green Algae (Cyanoprokaryotes) in Australian Freshwaters*; Cooperative Research Centre for Freshwater Ecology: Rockhampton, Australia, 2002.
35. Komárek, J. Chlorophyceae (Grünalgen), Ordnung: Chlorococcales. *Phytoplankt Süßwassers Syst. Biol.* **1983**, *7*.
36. Figler, A.; Dobronoki, D.; Márton, K.; Nagy, S.A.; Bácsi, I. Salt tolerance and desalination abilities of nine common green microalgae isolates. *Water* **2019**, *11*, 2527. [[CrossRef](#)]
37. Almutairi, A.W.; El-Sayed, A.E.-K.B.; Reda, M.M. Evaluation of high salinity adaptation for lipid bio-accumulation in the green microalga *Chlorella vulgaris*. *Saudi. J. Biol. Sci.* **2021**, *28*, 3981–3988. [[CrossRef](#)] [[PubMed](#)]
38. Kirrolia, A.; Bishnoi, N.R.; Singh, N. Salinity as a factor affecting the physiological and biochemical traits of *Scenedesmus quadricauda*. *J. Algal Biomass Util.* **2011**, *2*, 28–34.
39. Stanier, R.Y.; Kunisawa, R.; Mandel, M.; Cohen-Bazire, G. Purification and properties of unicellular blue-green algae (order Chroococcales). *Bacteriol. Rev.* **1971**, *35*, 171–205. [[CrossRef](#)]
40. Gan, X.; Shen, G.; Xin, B.; Li, M. Simultaneous biological desalination and lipid production by *Scenedesmus obliquus* cultured with brackish water. *Desalination* **2016**, *400*, 1–6. [[CrossRef](#)]
41. Ho, Y.S.; Ng, J.C.Y.; McKay, G. Kinetics of pollutant sorption by biosorbents: Review. *Sep. Purif. Methods* **2000**, *29*, 189–232. [[CrossRef](#)]
42. Weber, W.J.; Morris, J.C. Kinetics of Adsorption on Carbon from Solution. *J. Sanit. Eng. Div.* **1963**, *89*, 31–60. [[CrossRef](#)]
43. Koyuncu, I.; Sengur, R.; Turken, T.; Guclu, S.; Pasaoglu, M.E. Advances in water treatment by microfiltration, ultrafiltration, and nanofiltration. In *Advances in Membrane Technologies for Water Treatment*; Woodhead Publishing: Sawston, UK, 2015; pp. 83–128.
44. Christ, R.D.; Wernli, R.L., Sr. *The ROV Manual: A User Guide for Remotely Operated Vehicles, the Ocean Environment*; Butterworth-Heinemann: Oxford, UK, 2014; pp. 21–52.
45. Vakkilainen, E.K. *Steam Generation from Biomass: Construction and Design of Large Boilers*; Butterworth-Heinemann: Oxford, UK, 2017; pp. 180–202.
46. Christ, R.D.; Wernli, R.L., Sr. *The ROV Manual: A User Guide for Remotely Operated Vehicles, Vehicle Design and Stability*; Butterworth-Heinemann: Oxford, UK, 2014; pp. 107–120.
47. Nessim, R.B.; Tadros, H.R.Z.; Abou Taleb, A.E.A.; Moawad, M.N. Chemistry of the Egyptian Mediterranean coastal waters. *Egypt. J. Aquat. Res.* **2015**, *41*, 1–10. [[CrossRef](#)]
48. Kreitler, C.W. *Geochemical Techniques for Identifying Sources of Ground-Water Salinization*; CRC Press: Boca Raton, FL, USA, 1993.
49. Milroy, S. *Field Methods in Marine Science: From Measurements to Models*; Garland Science: New York, NY, USA, 2020.
50. Telahigue, F.; Agoubi, B.; Souid, F.; Kharroubi, A. Assessment of seawater intrusion in an arid coastal aquifer, south-eastern Tunisia, using multivariate statistical analysis and chloride mass balance. *Phys. Chem Earth Parts A/B/C* **2018**, *106*, 37–46. [[CrossRef](#)]
51. Shirazi, S.A.; Rastegary, J.; Aghajani, M.; Ghassemi, A. Simultaneous biomass production and water desalination concentrate treatment by using microalgae. *Desalin. Water Treat.* **2018**, *135*, 101–107. [[CrossRef](#)]
52. Sahle-Demessie, E.; Aly Hassan, A.; El Badawy, A. Bio-desalination of brackish and seawater using halophytic algae. *Desalination* **2019**, *465*, 104–113. [[CrossRef](#)]
53. Baghour, M. Algal degradation of organic pollutants. In *Handbook of Ecomaterials*; Springer: New York, NY, USA, 2019; pp. 565–586.

54. Min, M.; Hu, B.; Zhou, W.; Li, Y.; Chen, P.; Ruan, R. Mutual influence of light and CO₂ on carbon sequestration via cultivating mixotrophic alga *Auxenochlorella protothecoides* UMN280 in an organic carbon-rich wastewater. *J. Appl. Phycol.* **2012**, *24*, 1099–1105. [[CrossRef](#)]
55. Yang, K.-L.; Ying, T.-Y.; Yiacoumi, S.; Tsouris, A.C.; Vittoratos, E.S. Electrosorption of ions from aqueous solutions by carbon aerogel: An electrical double-layer model. *Langmuir* **2001**, *17*, 1961–1969. [[CrossRef](#)]
56. Shetty, P.; Gitau, M.M.; Maróti, G. Salinity stress responses and adaptation mechanisms in eukaryotic green microalgae. *Cells* **2019**, *8*, 1657. [[CrossRef](#)] [[PubMed](#)]
57. Yokoya, N.S.; De-Oliveira, E.C. Effects of salinity on the growth rate, morphology and water content of some Brazilian red algae of economic importance. *Cienc. Mar.* **1992**, *18*, 49–64. [[CrossRef](#)]
58. Ferroni, L.; Baldisserotto, C.; Pantaleoni, L.; Billi, P.; Fasulo, M.P.; Pancaldi, S. High salinity alters chloroplast morphology in a freshwater *Kirchneriella* species (Selenastraceae) from Ethiopian Lake Awasa. *Am. J. Bot.* **2007**, *94*, 1972–1983. [[CrossRef](#)] [[PubMed](#)]
59. Gautam, S.; Kapoor, D. Application of halophilic algae for water desalination. In *Handbook of Algal Biofuels*; Elsevier: Amsterdam, The Netherlands, 2022; pp. 167–179.